2019

Direct analysis of calcium in liquid infant formula via laser-induced breakdown spectroscopy (LIBS)

Xavier Cama-Moncunill

Maria Markiewicz-Keszycka

Patrick J. Cullen

See next page for additional authors

Funder: Department of Agriculture, Food and the Marine of Ireland

Authors

Xavier Cama-Moncunill, Maria Markiewicz-Keszycka, Patrick J. Cullen, Carl Sullivan, and Maria Piedad Casado-Gavalda

Food Chemistry 309 (2020) 125754

Contents lists available at ScienceDirect

Food Chemistry

journal homepage: www.elsevier.com/locate/foodchem

Direct analysis of calcium in liquid infant formula via laser-induced breakdown spectroscopy (LIBS)

Xavier Cama-Moncunill[a], Maria Markiewicz-Keszycka[a,*], Patrick J. Cullen[a,b], Carl Sullivan[a], Maria P. Casado-Gavalda[a]

[a] School of Food Science and Environmental Health, Technological University Dublin, Cathal Brugha St, Dublin 1, Ireland
[b] School of Chemical and Biomolecular Engineering, University of Sydney, Sydney, Australia

ARTICLE INFO

Keywords:
LIBS
Liquid analysis
Ready-to-feed infant formula
Calcium
PLSR

ABSTRACT

The present work illustrates the potential of laser-induced breakdown spectroscopy (LIBS) for the direct analysis of liquid food products. The aim of the experiment was to predict calcium content in ready-to-feed infant formula. The analysis was performed by a LIBS system coupled to a liquid sample chamber with a rotatory wheel that presents the liquid to the laser beam as a thin film. Multivariate analysis with partial least squares regression (PLSR) was performed to correlate LIBS spectral data to reference calcium contents. The obtained PLSR model exhibited a good fit and linearity, as indicated by the coefficients of determination for calibration (R_c^2) and cross-validation (R_{cv}^2), with values of 0.96 and 0.89, respectively. The robustness of the calibration model was assessed by external validation showing a root-mean-square error of prediction of 6.45 mg 100 mL^{-1}. These results demonstrated the potential of LIBS for real-time analysis of liquid food products.

1. Introduction

Infancy is a crucial phase of growth and development which requires appropriate nutrition. Breast milk is considered as the ideal food for infants (WHO, 2018); it provides the adequate amounts of nutrients for growth, as well as other substances with added health benefits. However, for numerous reasons breastfeeding might be either supplemented or replaced with breast milk substitutes. Infant formula (IF) is an industrially produced food designed to fulfil the nutritional requirements of infants during the first six months of life (Silva, Brandao, Matos, & Ferreira, 2015). In this regard, IF contains all the essential components: proteins, lipids, carbohydrates, minerals, and vitamins, in addition to other substances with particular nutritional purposes. To ensure the nutritional safety and adequacy of infant products, the amounts of all these components must be in conformity with national regulatory bodies such as the European Commission in the European Union, the Food and Drug Administration (FDA) in the United States, or the Codex Alimentarius Commission at an international level (Montagne, Van Dael, Skanderby, & Hugelshofer, 2009). Therefore, minimum and maximum contents of nutrients in IFs are clearly specified according to accepted scientific evidence (European Commission, 2016; Joint FAO/WHO Codex Alimentarius Commission, 2007).

Typically, IFs are commercially available in powder form. Liquid formulas, including ready-to-feed infant formula (RTF-IF) and liquid concentrates, are increasingly found in the market. Although liquid formulas account for a small volume of the global IF sales, mainly due to a higher retail price, the ready-to-feed format may be preferred in certain situations (Happe & Gambelli, 2015). It represents a convenient and hygienic option as it does not require preparation before consumption. Moreover, sterile RTF-IF are the predominant choice for feeding pre-term, low-birth-weight or immunocompromised infants (Happe & Gambelli, 2015; Marino, Meyer, & Cooke, 2013).

As previously mentioned, minerals are essential components of IF and indispensable for normal infant growth. Among other examples, minerals contribute to bone, brain and visual development. Calcium, which is the second most abundant mineral in IF and the most abundant mineral in the body, is involved in a wide variety of biological processes including growth and bone formation (Bae & Kratzsch, 2018). Since IF may be the only source of calcium for infants, it is of vital importance to ensure that its content lies within the regulatory range.

Conventional off-line techniques used in the analysis of minerals and trace elements in infant formulas such as atomic absorption spectroscopy (AAS), inductively coupled plasma optical emission spectroscopy (ICP-OES) or inductively coupled plasma mass spectroscopy (ICP-MS) often require long sample preparation procedures which also involve the use of chemicals such as acids or gases (dos Santos Augusto,

* Corresponding author.
E-mail address: maria.kesz@gmail.com (M. Markiewicz-Keszycka).

https://doi.org/10.1016/j.foodchem.2019.125754
Received 18 April 2019; Received in revised form 13 October 2019; Accepted 19 October 2019
Available online 23 October 2019

Barsanelli, Pereira, & Pereira-Filho, 2017; Ruiz, Ripoll, Hidalgo, & Canals, 2019). Despite the high sensitivity and accuracy of these methods, industries may benefit from the application of on-line/at-line technologies with real-time monitoring capabilities due to their speed, ease of operation and high sampling rates.

Laser-induced breakdown spectroscopy (LIBS) has been defined as a versatile real-time technique which allows *in-situ* analysis of any sort of material regardless of its physical state (Lazic & Jovićević, 2014). In the area of food analysis, LIBS has been gaining attention and the number of publications found in the literature has grown remarkably in the last few years (Fortes & Laserna, 2010; Senesi, Cabral, Menegatti, Marangoni, & Nicolodelli, 2019). To date, publications employing the technique for both qualitative and quantitative analysis of elements in various solid food samples can be found throughout the literature (Markiewicz-Keszycka et al., 2017). However, less attention has been paid to liquid food samples, especially with regard to direct analysis.

LIBS configurations for the analysis of liquids have been reported, e.g. liquid jets for Cr determination in industrial wastewater (Rai & Rai, 2008), double-pulse LIBS in bulk water (Giacomo, Dell'Aglio, Colao, Fantoni, & Lazic, 2005), and liquid surface analysis of formulations containing sodium chloride (St-Onge, Kwong, Sabsabi, & Vadas, 2004); nevertheless it has also been discussed that the direct analysis of liquids may be problematic. The reason for this is due to undesired effects such as shorter plasma durations, splashing, and formation of shockwaves on the liquid surface, which consequently lower the sensibility and repeatability of LIBS measurements (Rai, Yueh, & Singh, 2007; Sezer, Bilge, & Boyaci, 2017; St-Onge et al., 2004).

In the area of food analysis, the transformation of liquids into solid-matrix samples has been proposed. To do so, authors have employed the use of lyophilization techniques to remove the water content from milk samples (Moncayo, Manzoor, Rosales, Anzano, & Caceres, 2017), the formation of solid gel matrices by adding a binding agent such as collagen to milk (Sezer et al., 2018) and wine samples (Moncayo, Rosales, Izquierdo-Hornillos, Anzano, & Caceres, 2016), or the deposition of maternal milk and IF preparations (reconstituted powder) onto ashless filter papers (Abdel-Salam, Al Sharnoubi, & Harith, 2013). Alternatively, the formation of aerosols using sprayers for the quantification of calcium in milk has also been reported (Bilge, Sezer, Boyaci, Eseller, & Berberoglu, 2018). These techniques although obtaining improved results, required additional long sample preparation steps, which impeded real-time analysis.

In this study, the calcium content in RTF-IF samples was determined using a LIBS system equipped with a sample chamber designed for the direct analysis of liquids. Multivariate analysis with partial least squares regression (PLSR) was employed to develop a calibration model to reliably predict calcium content. LIBS measurements with different laser energy outputs were also performed and evaluated. The aim of this study was to assess the ability of LIBS for calcium content determination in RTF-IF, as well as illustrate its potential for the direct analysis of liquid foods.

2. Material and methods

2.1. Sample preparation

RTF-IF and ready-to-feed follow-on formula (RTF-FOF, formulas intended for children over 6 months of age) were acquired from local stores in Dublin, Ireland.

A total of three sample batches were prepared for calibration, each batch consisting of five samples (C1–C5) with varying content of calcium equally distributed in the range of approx. 10–90 mg 100 mL^{-1}. This range was intended to approximately cover the regulatory guidelines of the Codex Alimentarius Commission for calcium concentration in RTF-IF (Joint FAO/WHO Codex Alimentarius Commission, 2007). To prepare samples with different calcium contents, RTF-IF was mixed with calcium chloride (anhydrous, 97%, Lancaster Synthesis, Morecambe, UK) or distilled water to increase or decrease the calcium content in the mixtures, except for sample C3 which consisted of unmodified RTF-IF. Calculations required for sample preparation were made on the basis of the calcium contents provided by the manufacturers. To ensure reproducibility, each of the three batches was obtained from different RTF-IF bottles and prepared on different days.

Aiming to test the predictive ability of the calibration models, two validation samples were prepared with calcium contents differing to those of the calibration samples (V1, approx. 20 mg 100 mL^{-1}; V2, approx. 60 mg 100 mL^{-1}). Additionally, RTF-FOF was used as an extra validation sample (V3, approx. 70 mg 100 mL^{-1}) to assess the ability of the models for predicting calcium content in formulas with different composition. All samples were prepared in triplicates, giving a total number of 54 samples.

2.2. Atomic absorption spectroscopy (AAS)

Reference Ca contents for all 54 samples were established with a Varian 55B AA spectrometer (Varian Inc., Palo Alto, CA, USA). Sample digestion was carried out using a microwave system (MARS 6, CEM Corporation, Matthews, NC, USA). Approx. 1 g of each sample was weighed directly into a microwave vessel (MARSXpress, CEM Corporation), and filled with 10 mL nitric acid (HNO_3 69%, Sigma-Aldrich Ireland Ltd., Arklow, Ireland). Vessels were gently swirled and left open for 15 min to allow sample pre-digestion. The microwave heating program consisted of 2 steps: ramping from ambient temperature to 200 °C over 15 min (power set at 900 W), and holding that temperature for 15 additional minutes. After cooling, the digested solutions were transferred to 50 mL volumetric flasks and subsequently diluted with distilled water. A further dilution step using 25 mL flasks was carried out to bring Ca concentrations within the linear range of the instrument (0–3 ppm).

Calibration of the AA instrument was performed using five standard solutions prepared from a commercial calcium ion standard for AAS (1,000 mg L^{-1}, Sigma-Aldrich Ireland Ltd.), together with a blank solution, covering the range of 0–3 ppm. Calcium absorbance was measured at 422.7 nm with a slit width of 0.5 nm.

The three calibration batches were measured individually on different days (validation samples were measured along with the first batch).

2.3. LIBS instrumentation

Spectra of liquid samples were recorded using a LIBS-6 system (Applied Photonics Ltd., Skipton, UK) which comprised a 150 mJ Q-switched Nd:YAG laser (Nano SG 150–10, Litron lasers Ltd., Rugby, UK) and pulse duration of 5 ns coupled with six spectrometers (AvaSpec, Avantes BV, Apeldoorn, Netherlands) covering the wavelength range of 181–904 nm. The full width at half maximum (FWHM) ranged from 0.06 nm for the deep ultraviolet (UV) range to 0.18 nm for the visible near infrared (Vis-NIR) range. The system was fitted with a liquid chamber (SC-LQ2, Applied Photonics Ltd.) consisting of a rotatory nickel-plated stainless-steel wheel and a liquid reservoir of approximately 40 mL capacity.

A schematic representation of both the LIBS system and liquid chamber used in the experiments is shown in Fig. 1. To present liquids to the laser, the rotating wheel is partially submerged in the liquid forming a thin film on the exposed region as it emerges from the liquid bulk. This way, the film is constantly replenished at the lower part, and presented to the laser beam on the upper part where the laser is brought to focus. To improve the repeatability of experiments, the thickness and uniformity of the liquid film can be stabilized with the use of a gas purge jet directed at the wheel surface, beneath the focal plane of the laser. In the experiment, the sample chamber was coupled to an air pump (AP4, Interpet, Dorking, UK). The incoming flow of air gas uniformly distributed the thickness of the liquid film on the surface of the

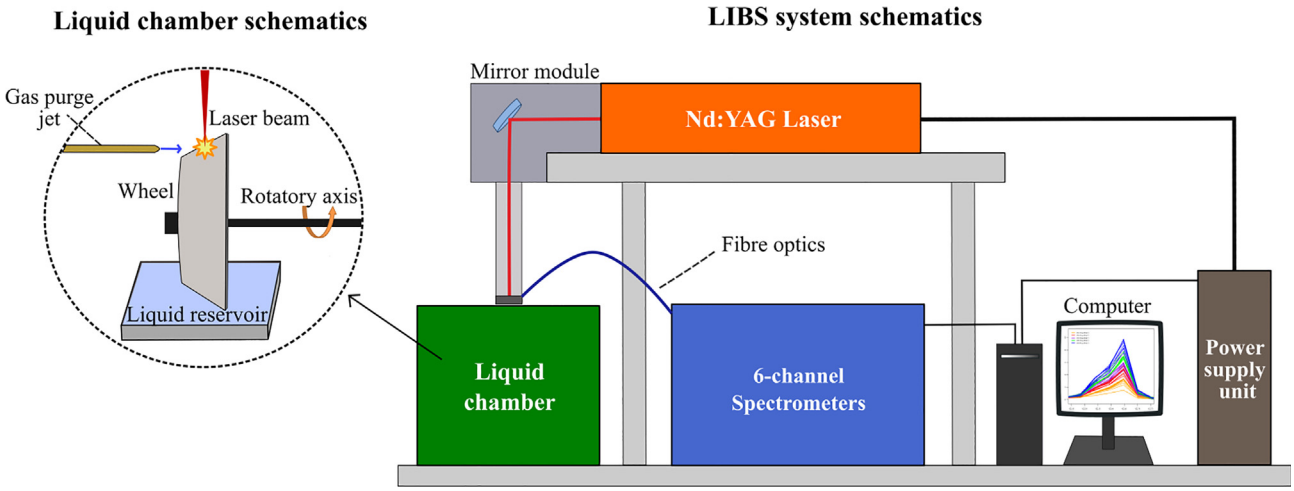

Fig. 1. Schematic representation of the LIBS system and liquid chamber used in the experiments.

rotating wheel where the laser beam was directed.

Another feature of the system is variable laser energy output which can be remotely controlled by changing the flashlamp Q-switched delay on the LIBS software interface (LIBSoft V16.4.1, Applied Photonics Ltd.).

2.3.1. Measurements

For LIBS analysis, samples were measured individually by pouring approximately 40 mL into the liquid reservoir. Both the reservoir and the wheel were thoroughly rinsed with distilled water before the analysis of each sample. Three different energy measurements with an output of 50, 100, and 150 mJ were performed and their resulting spectra recorded. Plasma emission was analyzed with a delay time of 1.27 μs and an integration time of 1.1 ms.

Preliminary testing was conducted to determine the optimum values for the following parameters: number of laser shots, repetition rate, rotational speed of the wheel, and film position relative to the focal plane of the laser beam. It was observed that accumulating a high number of laser shots produced better spectra in terms of signal-to-noise ratio. Thus, spectral acquisition was carried out by recording 200 consecutive laser shots (accumulations) for each energy measurement, giving a total number of 600 shots per sample. The laser was operated at a repetition rate of 2 Hz, and the rotatory wheel was set to revolve at an approximate speed of 1.26 rad/s (12 rpm). The position of the liquid film relative to the focal plane was adjusted manually using a micrometer control knob located at the sample chamber side. The final position was established based on a high sample signal and low wheel signal contribution, namely Ni I emission due to ablation of the wheel's surface material (see section 3.2).

Also, as seen for AAS, each of the three calibration batches was measured with LIBS individually on different days (validation samples were measured together with the first batch).

2.4. Data analysis

Univariate and multivariate data analysis were performed with R (R Core Team, 2016), along with the R package "pls" (Mevik, Wehrens, & Liland, 2016) for PLSR (partial least square regression) modelling.

Univariate analysis was conducted by means of simple linear regression (SLR) at 422.67 nm (Ca I); correlating LIBS signal intensities to the AAS measured Ca content of all 3 batches intended for calibration (N = 45).

Prior to PLSR, several pre-processing techniques were applied to the spectra with the aim of reducing undesired sources of signal fluctuations. Among the pre-processing techniques assessed, spectral normalization against the H I spectral line at 656.29 nm was selected based on PLSR-model performance. This normalization approach was found to provide suitable calibration curves in a previous publication (Cama-Moncunill et al., 2018). Firstly, data were divided into a calibration set (N = 45) used to develop the calibration curve, and a validation set (N = 6) to assess the robustness of the calibration. RTF-FOF (N = 3) was employed separately to assess the feasibility of the model for predicting calcium content in products with different composition (extra validation set). The fit and robustness of the PLSR model were evaluated by the coefficients of determination and root-mean-square errors for calibration (R_c^2, RMSEC), cross-validation (R_{cv}^2, RMSECV) and prediction (R_p^2, RMSEP). RMSE values were calculated as shown in Eq. (1) (El Haddad, Canioni, & Bousquet, 2014):

$$RMSE = \sqrt{\frac{\sum_{i=1}^{N} (\hat{y} - y_i)^2}{N - k}} \quad (1)$$

where $\hat{y}$ and y_i refer to the measured and predicted concentration values, respectively; N the number of samples in the dataset, and k the number of estimated parameters used in the computation of RMSE.

3. Results and discussion

3.1. AAS

Calibration of the AAS instrument was performed prior to the analysis of each batch. Good linearity was observed for the calibration curves rendering coefficient of determination values of ≥0.99. Detailed concentrations of calcium in the RTF-IF mixtures established with AAS are presented as Supplementary material in Table S1. Results show concentrations between batches slightly differ as some variability would be expected; this in turn helps building a robust calibration where variability is taken into account.

3.2. Laser energy and spectral features

An initial evaluation of the collected spectra was carried out to establish the principal differences between the three energy levels used, as well as to identify the main elemental emission lines in the spectra.

Fig. 2 shows the LIBS spectra acquired from the pure RTF-IF (sample C3, batch 1) using the three laser-shot energies 50, 100, and 150 mJ. Several of the most important spectral lines of elements occurring in the spectra can be seen. The main element emission lines in the spectra were identified using the NIST database (Kramida, Ralchenko, Reader, & NIST ASD team, 2016). These emission lines included: Ca II 393.37, 396.85 nm; Ca I 422.67 nm; H I 656.29 nm; N I 744.23, 746.83,

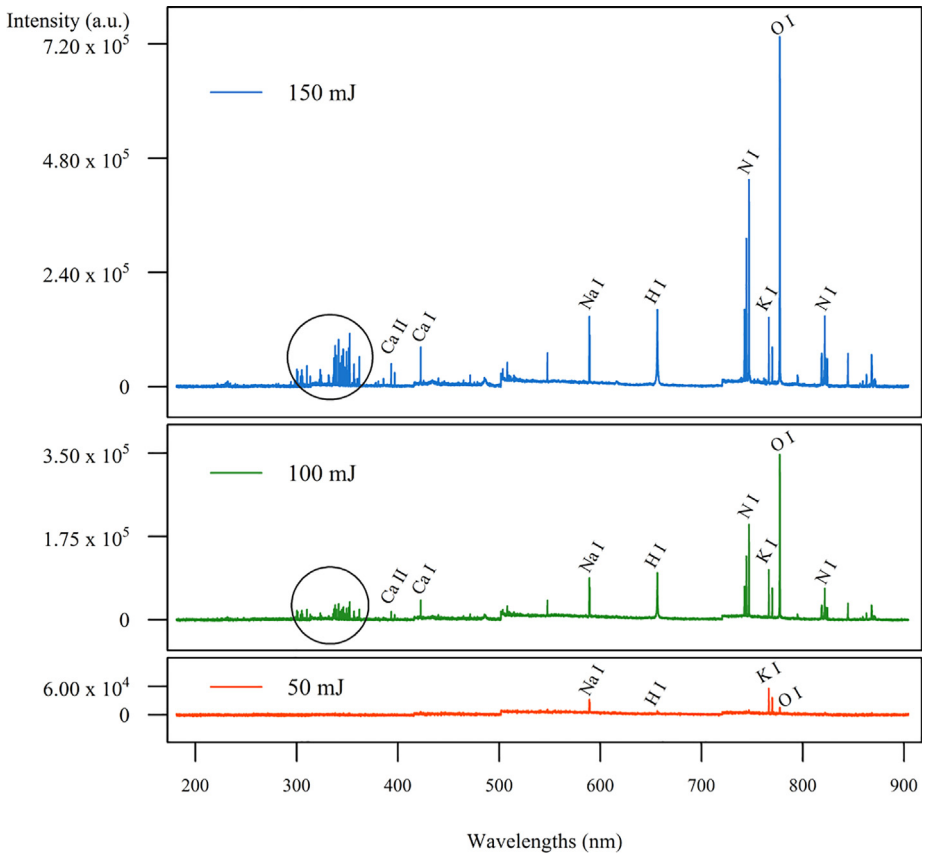

Fig. 2. LIBS spectra of RTF-IF (sample C3, 31.88 mg Ca 100 mL^{-1}) acquired with different laser energy outputs: from bottom to top, 50 mJ, 100 mJ and 150 mJ. Circles indicate areas of probable wheel contribution.

821.63 nm; K I 766.49, 769.90 nm; O I 777.19 nm; and Na I 589.05, 589.59 nm. The presence of several emission lines, namely Ni I, in the wavelength range from approx. 300 to 370 nm was attributed to ablation of wheel surface material (nickel plating). Ni I emission lines were identified at 300.25, 301.20, 305.08 310.16, 341.48, 345.85, 349.30, 352.46, 356.64, and 361.94 nm.

It can be seen in the Fig. 2 that the signal intensity increased with increasing laser energy, thus the spectra recorded with 150 mJ exhibited the highest overall intensity. The same pattern was observed for spectra collected from all other samples (not included in the Fig. 2 for clarity purposes). Several emission lines occurring in the 100 and 150 mJ spectra had marginal intensities in the 50 mJ measurement, including the Ca II lines within the wavelength range 393–397 nm and the Ca I line at 422.67 nm. With these experimental conditions, a pulse energy of 50 mJ may not be high enough to ablate and vaporize a sufficient amount of material to produce a strong emission signal of calcium lines.

A comparison between relative standard deviations of the intensities of samples at 422.67 nm using the three energy levels is presented in Fig. 3. The energy level of 150 mJ provided better results for quantification as relative standard deviations (RSD) were lower than those obtained for 100 and 50 mJ. Taking into account the results presented in Fig. 2 and Fig. 3, the energy level of 150 mJ was established as the optimum level for best results and therefore the following sections were applied on the data obtained at 150 mJ laser energy.

For comparison, it must be noted that the RSD values obtained for AAS measurements ranged from 2 to 5% depending on the concentration assessed, while for LIBS they were higher and ranged from 4.5 to 15%. However, for LIBS analysis, samples were analysed integrally without previous sample digestion.

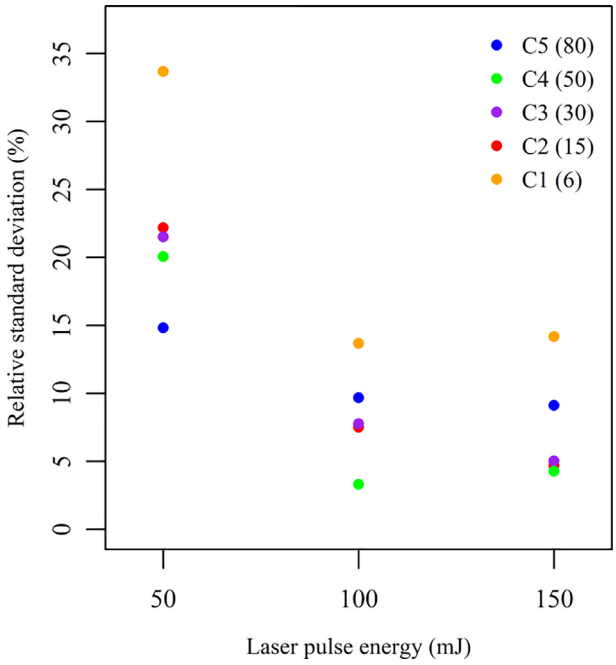

Fig. 3. Relative standard deviations for each sample at 422.67 nm corresponding to the three energy measurements: 50, 100, 150 mJ. Numbers between brackets indicate approx. calcium content in mg 100 mL^{-1} (N = 9).

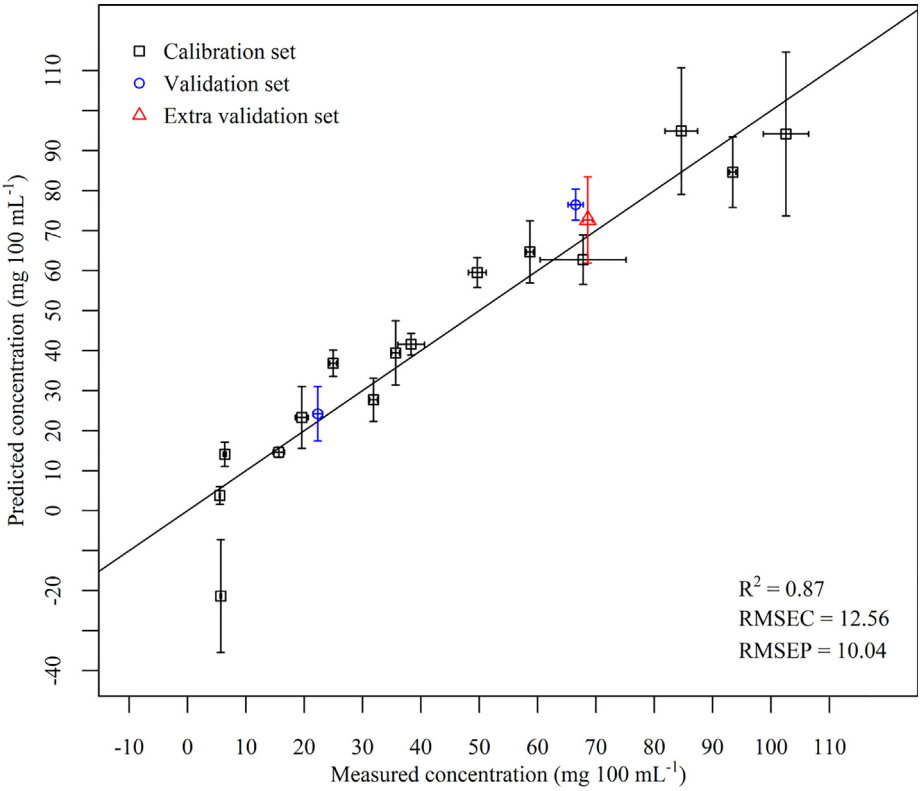

Fig. 4. Simple linear regression curve at 422.67 nm for batch 1 samples. RMSE values are expressed in mg 100 mL^{-1}.

Table 1
PLS-model performance in terms of R^2 (coefficients of determination) and RMSE (root-mean-square error) values for calibration, LOO cross-validation, and external validation using the validation data set.

No. LVs	Calibration (N = 45)		Cross-validation		Validation (N = 6)	
	R_c^2	RMSEC[a]	R_{cv}^2	RMSECV[a]	R_p^2	RMSEP[a]
2	0.66	18.36	0.59	20.16	0.14	20.48
3	0.86	11.89	0.80	13.98	0.89	7.43
4	0.96	6.56	0.89	10.23	0.91	6.45
5	0.99	3.20	0.88	10.69	0.92	6.23

[a] Expressed in milligrams per 100 ml.

3.3. Univariate analysis

An examination of the calcium emission lines indicated that spectra at 422.67 nm (Ca I) were correctly arranged according to their calcium content. Therefore, SLR (simple linear regression) at 422.67 nm was conducted, correlating signal intensities to the AAS-measured calcium contents.

Reasonable linearity was observed for SLR comprising of the three calibration batches (N = 45), exhibiting a coefficient of determination for calibration (R_c^2) of 0.87 and RMSEC of 12.56 mg 100 mL^{-1}. A calibration curve showing predicted versus measured Ca contents for all batches is presented in Fig. 4. The regression coefficients of the calibration curve were employed to predict Ca content in samples V1, V2 (validation set) and V3 (extra validation sample) which were observed to fit close to the calibration curve as expected.

Calibration curves fitting batches individually (N = 15), provided better linearity with R^2 values in the range of 0.92–0.93 depending on the batch used. This result suggests that variability from batch to batch limited the performance of the regression.

With the goal of improving the fit and accuracy of the regression, multivariate analysis with PLS and spectral pre-processing were explored.

3.4. PLS modelling

3.4.1. Model development and cross-validation

In order to develop a suitable calibration curve, spectra were normalized using the H I spectral line at 656.29 nm as internal standard and multivariate analysis was carried out. PLSR together with leave-one-out (LOO) cross-validation were applied to data corresponding to the three calibration batches. The wavelength area showing the probable wheel contribution (300–370 nm) was not included for PLSR. Although removing these wavelengths did not considerably impact the model performance, it slightly improved the results of R^2 and RMSE, especially concerning cross-validation.

LOO cross-validation was carried out to evaluate the performance of the models and determine the optimum number of latent variables (LV) (Cremers & Radziemski, 2013). The number of LVs to include for calibration was established based on the RMSECV (root-mean square error of cross-validation). The PLSR model included 4 LVs since the RMSECV resulted in a minimum value of 10.23 mg 100 mL^{-1} (Table 1). This number of LVs explained approx. 95% of the total variance of the model.

The calibration model exhibited suitable linearity shown by an R_c^2 of 0.96, which considerably improved the result obtained for univariate analysis (R_c^2 of 0.87 using three batches for calibration). When assessed by cross-validation, an R_{cv}^2 value of 0.89 was obtained, indicating a good fit for the PLS model.

3.4.2. Validation of the calibration model

As previously mentioned, validation was carried out to test the ability of the model to predict the Ca content of samples not included in the calibrations. Specifically, normalized spectral data of samples V1 and V2, with Ca contents of 22.32 and 66.53 mg 100 mL^{-1} respectively, were used for validation. Additionally, an extra validation sample V3, with Ca content of 68.61 mg 100 mL^{-1} was predicted to assess the

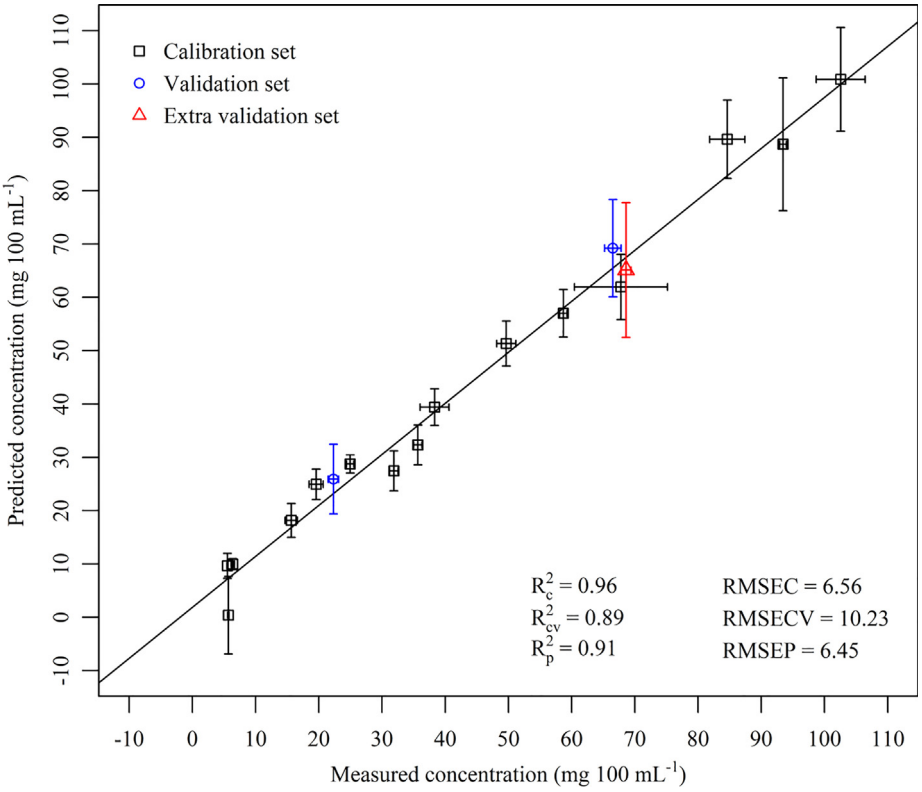

Fig. 5. PLS model built with the spectral data normalised by the H I 656.29 nm emission line corresponding to the calibration set (N = 45). The graph also shows the predicted Ca contents for the validation (V1 and V2) and extra validation (V3) sets. RMSE values are expressed in mg 100 mL^{-1}.

ability of the models for predicting calcium content in formulas with different composition.

The PLS calibration curve as well as the predicted concentrations of the validation set and extra validation with sample V3 are presented in Fig. 5. The y-axis shows the PLSR predicted concentrations, and the x-axis the reference Ca contents established by AAS. Ca contents and standard deviation values are in mg per 100 mL. In this figure, it can be observed that the highest and lowest Ca content samples (C1 and C5) presented higher standard deviations compared to that of the other samples. Lower accuracy for C1 and C5 measurements was also detected in the RSD values at 422.67 nm as shown in Fig. 3. Although this indicated that the concentration of these samples may be out of the optimum working range, the Ca content of sample C1 is below the minimum permitted level provided by the Codex Alimentarius Commission and C5 over the maximum.

When predicting the calcium contents of the validation set, the model exhibited a good predictive accuracy as corroborated by an R_p^2 of 0.91 and a RMSEP (root-mean square error of prediction) value of 6.45 mg 100 mL^{-1}.

Regarding the extra validation set consisting of RTF-FOF (ready-to-feed follow-on formula); the PLSR predicted calcium content was 65.10 mg 100 mL^{-1}, showing closeness to the measured value (68.61 mg 100 mL^{-1}). However, a high standard deviation of 12.64 mg 100 mL^{-1} (N = 3) was also observed for this measurement. The matrix or composition of follow-on formulas differ from that of IF, therefore, this result suggested that the model could still estimate the calcium concentration of products with a certain degree of variation.

In our previous work (Cama-Moncunill et al., 2017), the application of LIBS for calcium content determination in powdered IF was evaluated. Similarly, PLSR was employed to develop a quantitative model correlating LIBS spectra to reference Ca content. In that study, the PLSR models rendered a similar fit in terms of the R_c^2 and R_{cv}^2. The current work therefore proves that, despite the difficulties associated with the direct analysis of liquids, LIBS combined with PLSR analysis obtained as good results as the analysis of solid samples. The direct analysis of liquids can also provide advantages such as a greater homogeneity of the samples. Moreover, this method requires no sample preparation in comparison with powdered samples where a pellet is often required. This can be considerably beneficial for on-line/at-line applications in the industry, where small samples could be drawn from the process line directly to the system reservoir for analysis.

4. Conclusions

In this work, LIBS combined with multivariate analysis was successfully employed for quantifying the calcium content of RTF-IF samples. The direct analysis of liquids can be problematic due to a number of effects such as splashing or formation of ripples on the liquid surface, which, as a result, hinder the sensitivity and repeatability of LIBS experiments. Here, the use of a sample chamber designed for the direct analysis of liquids was proposed as a method for mineral quantification in liquid food samples. This sample chamber uses a rotatory wheel to present the sample in the form of a thin film to the laser beam. Also, it offers the advantage that the sample is constantly replenished as the wheel rotates, thus the laser can be repeatedly pulsed on new spots of the liquid film.

PLSR was carried out to develop a suitable calibration model for calcium content prediction in RTF-IF samples. The PLSR model obtained exhibited an R_c^2 of 0.96 and an R_{cv}^2 of 0.89, corroborating a good fit for the model. The RMSECV value was 10.23 mg 100 mL^{-1}. Validation of the calibration model was performed to test the robustness of the model obtaining an RMSEP value of 6.45 mg 100 mL^{-1}. The quality of the results were comparable to those obtained for food powdered samples, where the sample preparation of a pellet is normally required.

In general, the results obtained in this study illustrate the possibility of LIBS as a real-time tool for mineral analysis in liquid foods, with the added potential for at-line/on-line applications. LIBS gives an

advantage of fast measurements with a typical time analysis of one sample around 1–3 min. The technique is relatively inexpensive when compared with other methods based on optical emission spectroscopy. LIBS is also considered as environmentally friendly technique as it does not require any reagents and sample preparation steps. It is also relatively easy to use and safe for the operator when precautions and safety measures necessary when working with lasers are put in place.

Declaration of Competing Interest

The authors declare that they have no known competing financial interests or personal relationships that could have appeared to influence the work reported in this paper.

Acknowledgements

This work was supported by the Food Institutional Research Measure, administered by the Department of Agriculture, Food and the Marine of Ireland (Grant agreement: 14/F/866).

Appendix A. Supplementary data

Supplementary data to this article can be found online at https://doi.org/10.1016/j.foodchem.2019.125754.

References

Abdel-Salam, Z., Al Sharnoubi, J., & Harith, M. A. (2013). Qualitative evaluation of maternal milk and commercial infant formulas via LIBS. *Talanta, 115*, 422–426. https://doi.org/10.1016/j.talanta.2013.06.003.

Bae, Y. J., & Kratzsch, J. (2018). Vitamin D and calcium in the human breast milk. *Best Practice & Research Clinical Endocrinology & Metabolism, 32*(1), 39–45. https://doi.org/10.1016/J.BEEM.2018.01.007.

Bilge, G., Sezer, B., Boyaci, I. H., Eseller, K. E., & Berberoglu, H. (2018). Performance evaluation of laser induced breakdown spectroscopy in the measurement of liquid and solid samples. *Spectrochimica Acta Part B: Atomic Spectroscopy, 145*, 115–121. https://doi.org/10.1016/J.SAB.2018.04.016.

Cama-Moncunill, X., Markiewicz-Keszycka, M., Cama-Moncunill, R., Dixit, Y., Casado-Gavalda, M. P., Cullen, P. J., & Sullivan, C. (2018). Sampling effects on the quantification of sodium content in infant formula using laser-induced breakdown spectroscopy (LIBS). *International Dairy Journal, 85*, 49–55. https://doi.org/10.1016/J.IDAIRYJ.2018.04.014.

Cama-Moncunill, X., Markiewicz-Keszycka, M., Dixit, Y., Cama-Moncunill, R., Casado-Gavalda, M. P., Cullen, P. J., & Sullivan, C. (2017). Feasibility of laser-induced breakdown spectroscopy (LIBS) as an at-line validation tool for calcium determination in infant formula. *Food Control, 78*, 304–310. https://doi.org/10.1016/j.foodcont.2017.03.005.

Cremers, D. A., & Radziemski, L. J. (2013). *Handbook of laser-induced breakdown spectroscopy* (2nd ed.). Chichester, UK: John Wiley & Sons Ltd.

dos Santos Augusto, A., Barsanelli, P. L., Pereira, F. M. V., & Pereira-Filho, E. R. (2017). Calibration strategies for the direct determination of Ca, K, and Mg in commercial samples of powdered milk and solid dietary supplements using laser-induced breakdown spectroscopy (LIBS). *Food Research International, 94*, 72–78. https://doi.org/10.1016/j.foodres.2017.01.027.

El Haddad, J., Canioni, L., & Bousquet, B. (2014). Good practices in LIBS analysis: Review and advices. *Spectrochimica Acta Part B: Atomic Spectroscopy, 101*, 171–182. https://doi.org/10.1016/j.sab.2014.08.039.

European Commission. (2016). Commission Delegated Regulation (EU) 2016/127 of 25 September 2015. Official Journal of the European Union, L 25, 1–29.

Fortes, F. J., & Laserna, J. J. (2010). The development of fieldable laser-induced breakdown spectrometer: No limits on the horizon. *Spectrochimica Acta Part B: Atomic Spectroscopy, 65*(12), 975–990. https://doi.org/10.1016/J.SAB.2010.11.009.

Giacomo, A. De, Dell'Aglio, M., Colao, F., Fantoni, R., & Lazic, V. (2005). Double-pulse LIBS in bulk water and on submerged bronze samples. *Applied Surface Science, 247*(1–4), 157–162. https://doi.org/10.1016/J.APSUSC.2005.01.034.

Happe, R. P., & Gambelli, L. (2015). Infant formula. *Specialty Oils and Fats in Food and Nutrition, 285–315*. https://doi.org/10.1016/B978-1-78242-376-8.00012-0.

Joint FAO/WHO Codex Alimentarius Commission. (2007). CODEX STAN 72 – 1981 Standard for infant formula and formulas for special medical purposes intended for infants. Rome: Food and Agriculture Organization of the United Nations.

Kramida, A., Ralchenko, Y., Reader, J., & NIST ASD team. (2016). NIST Atomic Spectra Database (version 5.4). Retrieved December 4, 2017, from https://www.nist.gov/pml/atomic-spectra-database.

Lazic, V., & Jovićević, S. (2014). Laser induced breakdown spectroscopy inside liquids: Processes and analytical aspects. *Spectrochimica Acta Part B: Atomic Spectroscopy, 101*, 288–311. https://doi.org/10.1016/J.SAB.2014.09.006.

Marino, L. V., Meyer, R., & Cooke, M. L. (2013). Cost comparison between powdered versus energy dense infant formula for undernourished children in a hospital setting. *E-SPEN Journal, 8*(4), e145–e149. https://doi.org/10.1016/j.clnme.2013.04.002.

Markiewicz-Keszycka, M., Cama-Moncunill, X., Casado-Gavalda, M. P., Dixit, Y., Cama-Moncunill, R., Cullen, P. J., & Sullivan, C. (2017). Laser-induced breakdown spectroscopy (LIBS) for food analysis: A review. *Trends in Food Science & Technology, 65*, 80–93. https://doi.org/10.1016/j.tifs.2017.05.005.

Mevik, B.-H., Wehrens, R., & Liland, K. H. (2016). Partial least squares and principal component regression.

Moncayo, S., Manzoor, S., Rosales, J. D., Anzano, J., & Caceres, J. O. (2017). Qualitative and quantitative analysis of milk for the detection of adulteration by Laser Induced Breakdown Spectroscopy (LIBS). *Food Chemistry, 232*, 322–328. https://doi.org/10.1016/j.foodchem.2017.04.017.

Moncayo, S., Rosales, J. D., Izquierdo-Hornillos, R., Anzano, J., & Caceres, J. O. (2016). Classification of red wine based on its protected designation of origin (PDO) using Laser-induced Breakdown Spectroscopy (LIBS). *Talanta, 158*, 185–191. https://doi.org/10.1016/j.talanta.2016.05.059.

Montagne, D.-H., Van Dael, P., Skanderby, M., & Hugelshofer, W. (2009). 9 – Infant formulae – powders and liquids. In A. Y. Tamime (Ed.). *Dairy powders and concentrated products* (pp. 294–331). Oxford, UK: Blackwell Publishing.

R Core Team. (2016). R: A language and environment for statistical computing. https://doi.org/citeulike-article-id:708579.

Rai, V. N., Yueh, F. Y., & Singh, J. P. (2007). Chapter 10 – Laser-induced breakdown spectroscopy of liquid samples. Laser-Induced Breakdown Spectroscopy, 223–254. doi: 10.1016/B978-044451734-0.50013-2.

Rai, N. K., & Rai, A. K. (2008). LIBS—An efficient approach for the determination of Cr in industrial wastewater. *Journal of Hazardous Materials, 150*(3), 835–838. https://doi.org/10.1016/J.JHAZMAT.2007.10.044.

Ruiz, F. J., Ripoll, L., Hidalgo, M., & Canals, A. (2019). Dispersive micro solid-phase extraction (DμSPE) with graphene oxide as adsorbent for sensitive elemental analysis of aqueous samples by laser induced breakdown spectroscopy (LIBS). *Talanta, 191*, 162–170. https://doi.org/10.1016/J.TALANTA.2018.08.044.

Senesi, G. S., Cabral, J., Menegatti, C. R., Marangoni, B., & Nicolodelli, G. (2019). Recent advances and future trends in LIBS applications to agricultural materials and their food derivatives: An overview of developments in the last decade (2010–2019). Part II. Crop plants and their food derivatives. *TrAC Trends in Analytical Chemistry, 118*, 453–469. https://doi.org/10.1016/J.TRAC.2019.05.052.

Sezer, B., Bilge, G., & Boyaci, I. H. (2017). Capabilities and limitations of LIBS in food analysis. *TrAC Trends in Analytical Chemistry, 97*(Supplement C), 345–353. https://doi.org/10.1016/j.trac.2017.10.003.

Sezer, B., Durna, S., Bilge, G., Berkkan, A., Yetisemiyen, A., & Boyaci, I. H. (2018). Identification of milk fraud using laser-induced breakdown spectroscopy (LIBS). *International Dairy Journal, 81*, 1–7. https://doi.org/10.1016/J.IDAIRYJ.2017.12.005.

Silva, A. S., Brandao, G. C., Matos, G. D., & Ferreira, S. L. C. (2015). Direct determination of chromium in infant formulas employing high-resolution continuum source electrothermal atomic absorption spectrometry and solid sample analysis. *Talanta, 144*, 39–43. https://doi.org/10.1016/J.TALANTA.2015.05.046.

St-Onge, L., Kwong, E., Sabsabi, M., & Vadas, E. B. (2004). Rapid analysis of liquid formulations containing sodium chloride using laser-induced breakdown spectroscopy. *Journal of Pharmaceutical and Biomedical Analysis, 36*(2), 277–284. https://doi.org/10.1016/J.JPBA.2004.06.004.

WHO. (2018). Infant and young child feeding. Retrieved April 5, 2019, from http://www.who.int/en/news-room/fact-sheets/detail/infant-and-young-child-feeding.